

# $\phi$ meson electroproduction at low transferred momentum

Afraa A. Kanaan<sup>1\*</sup>, Khalid M. A. Hamad<sup>1</sup> and Ali A. Alzubadi<sup>3</sup>



Physics Department, College of Science, University of Anbar.

Ramadi ,Anbar ,Iraq<sup>1</sup>: e-mail [sc.af.ak33@uoanbar.edu.iq](mailto:sc.af.ak33@uoanbar.edu.iq)

<sup>1</sup>Physics Department, College of Science, University of Anbar.

Ramadi ,Anbar ,Iraq<sup>1</sup> e-mail Khalid [hamad2002@yahoo.com](mailto:hamad2002@yahoo.com)

<sup>3</sup>Physics Department, College of Science, University of Baghdad.

Jadirayha, Baghdad, Iraq :e-mail [ali.abdullatif@sc.uobaghdad.edu.iq](mailto:ali.abdullatif@sc.uobaghdad.edu.iq)

## ARTICLE INFO

Received: 18 / 09 / 2022

Accepted: 30 / 10 / 2022

Available online: 22 / 12 / 2022

DOI: [10.37652/juaps.2022.176471](https://doi.org/10.37652/juaps.2022.176471)

### Keywords:

$\phi$  vector mesons, pomeron

model, Regge pole;

Electroproduction,

Copyright©Authors, 2022, College of Sciences, University of Anbar. This is an open-access article under the CC BY 4.0 license (<http://creativecommons.org/licenses/by/4.0/>).



## ABSTRACT

The electroproduction of  $\phi$  meson is analyzed. The amplitude consist of two terms, the soft and the hard pomeron terms. it is assumed, that both pomerons are Regge poles. In the present approach, the two pomeron amplitude for the photoproduction processes is extended to construct an amplitude for the electroproduction processes by introducing the photon virtual mass ( $Q^2$ ). The residues of the two poles become functions of ( $Q^2$ ). These functions are extracted by fitting the differential cross section ( $\frac{d\sigma}{dt}$ ) of the extended model at constant energy( $w$ ) to the experimental data using the chi- square method. At each  $Q^2$ , the hard and the soft terms are multiplied by the factors  $C_0$  and  $C_1$  to match the data. The vertices of the pomeron coupling to the interacting particles are calculated by the dimensions of the vertices which are related to the masses of the interacting particles at each vertex.

## 1 Introduction

Diffraction electroproduction of a vector meson ( $V$ ) is represented by the process

$\gamma^* p \rightarrow V p$  (1) where  $V = \rho, \omega, \phi, J/\Psi \dots$  vector mesons

The main controlling variables are:  $Q^2$ ,  $t$  and  $m_v$ , with  $t$  is the squared of the transferred momentum and  $m_v$  is the meson mass. The hard region is reached if one of these variables is large[1,2]. In that case, the QCD calculations should be used [1-4]. Most of the qualitative properties of the data can be reproduced by such calculations. However, the calculations suffer from uncertainties in the gluon distribution and the vector meson wave function which introduces uncertainty in the overall normalization. Different models introduced  $Q^2$  dependence using different approaches. Some of these models assume that the coupling of pomeron to the photon-vector meson vertex is responsible for this dependence[1,5]. Some other models used the  $Q^2$  in the parameters of pomeron trajectory [5-6].

As the process in present case is elastic, the variable  $t$  is not a hard scale. Furthermore, the  $\phi$  mass is about  $1.02 \text{ GeV}$ , then the  $Q^2$  is the only hard variable [3]. The two pomeron model involves contributions from the hard and the soft terms. A transition from a soft regime to a hard regime in the process is set by  $Q^2$ . Data on the total cross section for the photoproduction at high  $w$  is parameterized as  $w^\delta$ [7-9]. The parameter  $\delta$  [10-11] increases as the mass scale ( $m_v^2$ ) increases while, for electroproduction [3]  $\delta$  increases with the hard scale ( $m_v^2 + Q^2$ ). However, the rate of increase of  $\delta$  decreases with increasing the hard scale [3,4]. The values of  $\delta$  can be obtained by fitting the total cross section using  $w^\delta$  at each  $Q^2$ . Experimentally, The differential cross section is parameterized as  $e^{-b|t|}$ , with  $b$  decreases from about  $12 \text{ GeV}^{-2}$  at small value of the hard scale to a universal scale value of about  $5 \text{ GeV}^{-2}$  as the hard scale increases[12].

## 2 Theoretical model

\*Corresponding author at Physics Department, College of Science, University of Anbar. Ramadi ,Anbar ,Iraq;  
E-mail address [sc.af.ak33@uoanbar.edu.iq](mailto:sc.af.ak33@uoanbar.edu.iq)

To derive an amplitude for vector meson production by a virtual photon in eq.(1), we extend the two pomeron amplitude for the photoproduction by introducing the virtual photon mass ( $Q^2$ ) to the amplitude[3,4 , 13-15], then:

$$T(s, t, Q^2, m_v^2) \approx if(t, Q^2, m_v^2) \left( \frac{m_v^2}{m_v^2 + Q^2} \right)^n [ A_0 \left( \frac{s}{s_0} \right)^{\alpha_{P_0}(t)-1} e^{-i\frac{\pi}{2}\alpha_{P_0}(t)} + A_1 \left( \frac{s}{s_1} \right)^{\alpha_{P_1}(t)-1} e^{-i\frac{\pi}{2}\alpha_{P_1}(t)} ] \quad (2)$$

with  $s = w^2$  is the total center of mass of energy squared.  $A_0$  and  $A_1$  are normalization constants in the photoproduction amplitude . The soft and the hard trajectories of the pomeron are taken here as:

$$\alpha_{P_1}(t) = 1.08 - \alpha_{P_1} |t| \quad (3)$$

$$\alpha_{P_0}(t) = 1.44 - \alpha_{P_0} |t| \quad (4)$$

with  $\alpha_{P_1} = 0.25$  and  $\alpha_{P_0} = 0.01$  are the slopes of the trajectories, while the energy scales are taken as[16]  $s_0 = \frac{1}{\alpha_{P_0}}$  and  $s_1 = \frac{1}{\alpha_{P_1}}$  . The  $f(t, Q^2, m_v^2)$  involves the forms of coupling of the trajectories to proton and photon-vector meson vertices. These forms are related to the dimensions of the vertices or to the radius of interaction ( $R^2$ ) of the particles. The dependence of the function on  $t$  should have an exponential as required by the data. Then the form of the function behaves like  $e^{-R^2|t|}$ . with  $R^2$  is a sum of the radii of the proton vertex ( $R_p^2$ ) and the photon-vector meson vertex ( $R_v^2(Q^2)$ ) [1,17] i.e:

$$R^2 = R_p^2 + R_v^2(Q^2) \quad (5)$$

These radii are related to the inverse of the masses of the interacting particles at each vertex. Then, the radius of the proton vertex is given by:

$$R_p^2 = 2 \text{ GeV}^{-2} \quad (6)$$

While, the photon-vector meson vertex is

$$R_v^2(Q^2) = \frac{R_{0v}^2 m_p^2}{m_v^2 + Q^2} \quad (7)$$

with  $R_{0v}^2 \text{ GeV}^{-2}$  is a fitting parameter ,  $m_p^2$  is the  $\rho$  meson mass. The largest radius of interaction is that of the real photon interaction, while the smallest radius is when  $Q^2$  is very large as given by eq.(7).

The function  $\left( \frac{m_v^2}{m_v^2 + Q^2} \right)^n$  in eq.(2) introduces the variation of the cross section with  $Q^2$  at a constant

energy [4]. The value of  $n$  may be deduced from the data. Extracting the slopes of the pomeron trajectories in the exponent of  $s$  in eq.(2), then the forward slope including eq.(5) should take the following forms for the soft and hard terms [1,4]:

$$\Lambda_0 = R^2 + \alpha_{P_0} \ln \left( \frac{s}{s_0} \right) \quad (8)$$

$$\Lambda_1 = R^2 + \alpha_{P_1} \ln \left( \frac{s}{s_1} \right) \quad (9)$$

Squaring eq.( 2) we get:

$$\frac{d\sigma}{dt} = R_T \left( \frac{m_v^2}{m_v^2 + Q^2} \right)^{2n} \left| A_0 \left( \frac{s}{s_0} \right)^{0.44} e^{-i\frac{\pi}{2}\alpha_{P_0}(t)} e^{-\Lambda_0 |t|} + A_1 \left( \frac{s}{s_1} \right)^{0.08} e^{-i\frac{\pi}{2}\alpha_{P_1}(t)} e^{-\Lambda_1 |t|} \right|^2 \quad (9)$$

where  $R_T = 1 + \frac{Q^2}{m_v^2}$

introduces the contribution from the longitudinal photons. The differential cross section for meson photoproduction can be obtained by setting  $Q^2 = 0$  in eq.(9). For electroproduction the soft and the hard terms eq.(9) should be multiplied by the factors  $C_0$  and  $C_1$  for the normalization with the data, then:

$$\frac{d\sigma}{dt} = R_T \left( \frac{m_v^2}{m_v^2 + Q^2} \right)^{2n} \left| C_0 * A_0 \left( \frac{s}{s_0} \right)^{0.44} e^{-i\frac{\pi}{2}\alpha_{P_0}(t)} e^{-\Lambda_0 |t|} + C_1 * A_1 \left( \frac{s}{s_1} \right)^{0.08} e^{-i\frac{\pi}{2}\alpha_{P_1}(t)} e^{-\Lambda_1 |t|} \right|^2 \quad (10)$$

Using the minimum ( $\chi^2$ ) method, these factors are adjusted by comparing eq.(10) with the experimental data [18-20]. It is found that all the  $\chi^2$  values are less than one. The resulting  $C_0$  and  $C_1$  factors are denoted by the weights. The initial guessed for the value of  $n$  in eq.(10) may be motivated by the form of the  $Q^2$  dependence of the experimental data. The obtained values for  $\varphi$  meson are ( $n = 1.36$  for  $Q^2 \leq 6.6$  and  $n = 1.4$  for otherwise). It is clear that the values of weights for photoproduction are  $C_0 = C_1 = 1.0$

### 3 Results

In the following the results of using the two pomeron model in calculating the electroproduction of  $\varphi$  vector meson is discussed.

#### 3.1 $\varphi$ meson electroproduction

Fitting the  $\frac{d\sigma}{dt} (\gamma^* p \rightarrow \varphi p)$  data[18] as a function of  $t$  at  $w = 75 \text{ GeV}$  for different values of  $Q^2$  using the model discussed above. The obtained values  $C_0$  and  $C_1$  at each  $Q^2$  are given in table (1).

**Table (1) the variations of the weights  $C_0$  and  $C_1$  at  $Q^2$**

$\frac{Q^2}{Q_0^2}$	$C_0$	$C_1$
2.4	1.13	0.99
3.6	1.25	0.95
5.2	1.35	0.86
6.9	1.5	0.85
12.6	1.6	0.83
19.7	1.65	0.55

The weights  $C_0$  as a function of  $Q^2$  are plotted in fig.1 (a) , while the weights  $C_1$  are plotted in fig. 1(b).

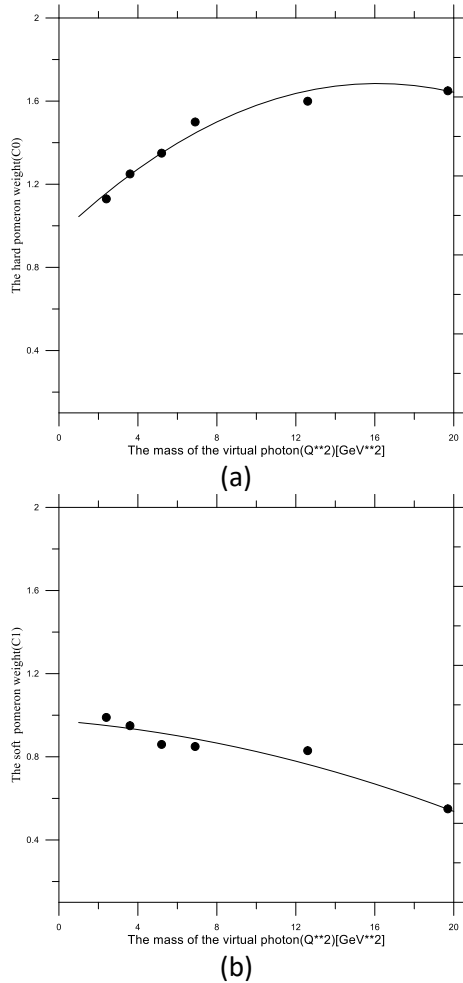


**Fig.(1) (a) Hard pomeron and (b) soft pomeron weights as functions of  $Q^2$**

The general behaviors of the fitting curves may be given by the forms:

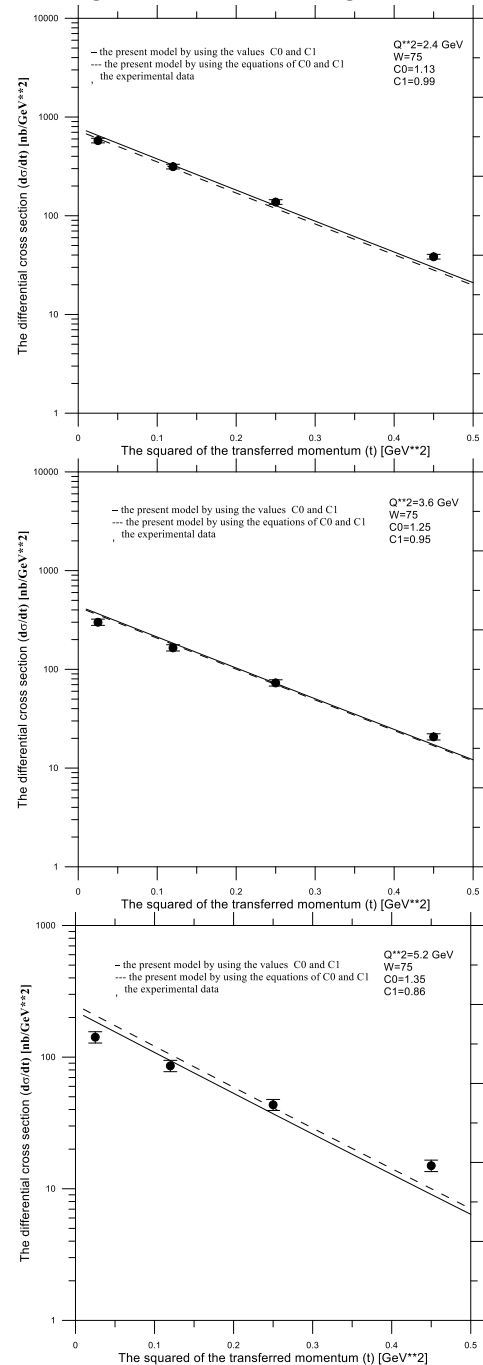
$$C_0 = -0.0028 * \left(\frac{Q^2}{Q_0^2}\right) + 0.0903 * \left(\frac{Q}{Q_0}\right) + 0.9567 \quad (11)$$

$$C_1 = -0.0007 * \left(\frac{Q^2}{Q_0^2}\right) - 0.0078 * \left(\frac{Q}{Q_0}\right) + 0.9734 \quad (12)$$

It is clear that the hard pomeron weights in fig.1(a) increases with  $Q^2$ , but the rate of the increase is decreasing with  $Q^2$ . Therefore, the curve may scale at large  $Q^2$ . As  $Q^2$  increases the hard weight dominates. On the other hand, the contribution from the soft pomeron is decreasing.

### 3.1.1 t dependence

The data [18] on the differential cross section  $\left(\frac{d\sigma}{dt}(\gamma^*p \rightarrow \varphi p)\right)$  as a function of  $t$  at  $w = 125 \text{ GeV}$  and for different  $Q^2$  values ( $Q^2=2.4, 3.6, 5.2, 6.9, 12.6$  and  $19.7 \text{ GeV}^2$ ) are shown in fig.(2). The data are compared with the results of the two pomeron model in eq. (10). The dashed curves are the results of the model using eqs.(11,12). A reasonable fit for the data in terms of the model is clear.  $\frac{d\sigma}{dt}$  decreases exponentially as  $e^{-b|t|}$  with,  $b$  can be obtained by fitting the data at each  $Q^2$ . Experimentally, it reduces with increasing  $Q^2$  and scales at large values of  $Q^2$ .



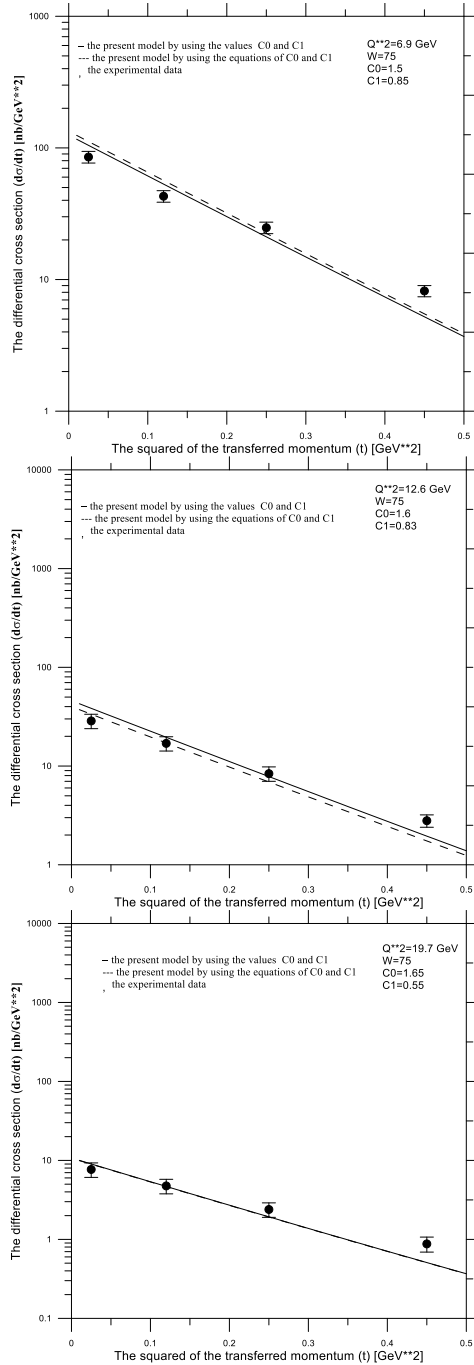


**Fig.(2)  $\frac{d\sigma}{dt}(\gamma^*p \rightarrow \phi p)$  for different  $Q^2$  at  $w = 75$  GeV [19]. The solid curves are the model, while the dashed curves are in terms of eqs.(11,12).**

### 3.1.2 $w$ dependence

The total elastic cross section is obtained by integrating eq. (10) over  $t$  from  $t=0$  to  $t=1.13$ . at different values of  $Q^2$  as shown in fig.(3). The results of the calculation are compared with the data [19] on the total cross section as a function of  $w$  in fig.(3) at values of different  $Q^2$  (2.4, 3.8, 6.5 and 13.  $GeV^2$ ). We notice the steep increase of the cross section with energy. As expected, the data rise like  $w^\delta$ . this form can be used to fit the data and to find the value of  $\delta$  at

each  $Q^2$ . An agreement between the model and the data is clear in fig.(3). The steep increase with energy at a constant  $Q^2$  is attributed to the high intercept of the hard pomeron trajectory.

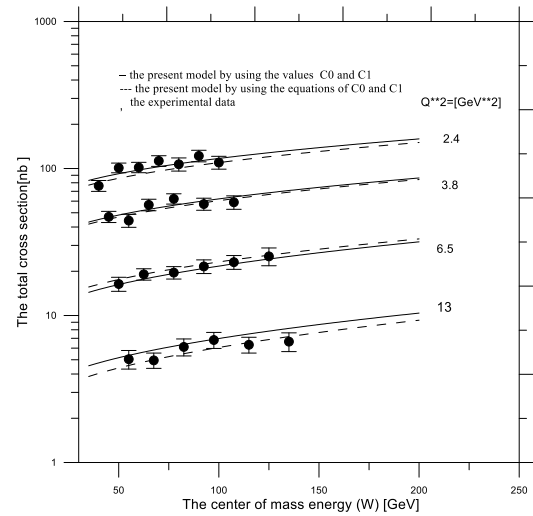


**Figure 3 : Total cross section as a function of  $w$  at different values of  $Q^2$  [19]. Solid curves are the model, while dashed curves are the model using eqs.(11,12) .**

## 4 Summery and Conclusions

The two pomeron model is used to calculate the electroproduction of phi meson. The photoproduction amplitude is extended by introducing the virtual photon mass to construct the electroproduction amplitude .In addition to the fitting factors found in photoproduction amplitude, the hard and soft pomeron terms must be multiplied by certain fitting factors known as weights. The minimal chi square approach may be used to progressively change these weights until the electroproduction data is well-fitted. Tables (1) for the Phi meson tabulate the weight values as a function of  $Q^2$ . The hard weight rises with  $Q^2$  and is predicted to scale large  $Q^2$  values. The model shows agreements with the data on the differential and total cross sections in figs.(2,3).

## References

- [1]Haakman, L. P. A., Alexei Kaidalov, and Justus H. Koch. "Production of vector mesons by real and virtual photons at high energies." Physics Letters B 365.1-4 (1996): 411-417.
- [2] Aktas, Adil, et al. "Diffractive deep-inelastic scattering with a leading proton at HERA." The European Physical Journal C-Particles and Fields 48.3 (2006): 749-766.

- [3] Hamad, Khalid MA, Maysoun K. Bunayi, and Afraa A. Kanaan. "Energy dependence of the electroproduction of vector mesons." *Indian Journal of Physics* 90.8 (2016): 937-942.
- [4] Hamad, Khalid, Maysoun K. Bunayi, and Afraa A. Kanaan. "One-pomeron model in vector mesons production." *The European Physical Journal A* 55.10 (2019): 1-8.
- [5] Jenkovszky, L. L., E. S. Martynov, and F. Paccanoni. "Regge pole model for vector meson photoproduction at HERA." *arXiv preprint hep-ph/9608384* (1996).
- [6] Martynov, E., Enrico Predazzi, and A. Prokudin. "A universal Regge pole model for all vector meson exclusive photoproduction by real and virtual photons." *The European Physical Journal C-Particles and Fields* 26.2 (2002): 271-284.
- [7] H1 Collaboration. "Elastic  $J/\psi$  production at HERA." *The European Physical Journal C-Particles and Fields* 46 (2006): 585-603.
- [8] Adloff, Catherine, et al. "Diffractive photoproduction of  $\psi$  (2S) mesons at HERA." *Physics Letters B* 541.3-4 (2002): 251-264.
- [9] Collaboration, Z. E. U. S., et al. "Exclusive photoproduction of  $\Upsilon$  mesons at HERA." *Phys. Lett. B* 680.4 (2009).
- [10] Aid, S., et al. "Elastic and inelastic photoproduction of  $J/\psi$  mesons at HERA." *Nuclear Physics B* 472.1-2 (1996): 3-31.
- [11] ZEUS Collaboration gallo@mail. desy. de. "Exclusive  $\rho^0$  production in deep inelastic scattering at HERA." *PMC Physics A* 1 (2007): 1-47.
- [12] Levy, Aharon. "Electroproduction of vector mesons." *arXiv preprint arXiv:0907.2178* (2009).
- [13] Donnachie, Alexander, and Peter V. Landshoff. "Exclusive vector meson production at HERA." *Physics Letters B* 348.1-2 (1995): 213-218.
- [14] Donnachie, Alexander, and Peter V. Landshoff. "Exclusive vector photoproduction: confirmation of Regge theory." *Physics Letters B* 478.1-3 (2000): 146-150.
- [15] Donnachie, Alexander, and P. V. Landshoff. "Successful description of exclusive vector meson electroproduction." *arXiv preprint arXiv:0803.0686* (2008).
- [16] Fazio, S., et al. "Reggeometry of deeply virtual Compton scattering (DVCS) and exclusive vector meson production (VMP) at HERA." *arXiv preprint arXiv:1304.1891* (2013).
- [17] Bunyatyan, Armen. "Exclusive vector mesons and DVCS at HERA." *Nuclear Physics B (Proceedings Supplements)* 179 (2008): 69-77.
- [18] Aaron, Francise D., et al. "Diffractive electroproduction of  $\rho$  and  $\phi$  mesons at HERA." *Journal of High Energy Physics* 2010.5 (2010): 1-111.
- [19] Chekanov, S., et al. "Exclusive electroproduction of  $J/\psi$  mesons at HERA." *Nuclear Physics B* 695.1-2 (2004): 3-37.
- [20] Piotrowska, Milena. "Study of conventional and non-conventional scalar and vector mesons." *arXiv preprint arXiv: 2105. 08557* (2021).

## الانتاج الكهربائي للفأى ميزون بزخم منقول منخفض

عفرأ عماش كنعان<sup>1</sup> , خالد محمد عبد<sup>1</sup> , علي عبداللطيف كريم<sup>2</sup>

<sup>1</sup> قسم الفيزياء , كلية العلوم , جامعة الأنبار

<sup>2</sup> قسم الفيزياء , كلية العلوم , جامعة بغداد

### الخلاصة:

يتم تحليل الإنتاج الكهربائي لفأى ميزون. المكونات اللذان يشكلان السعة هما مصطلحات بوميرون الناعمة والصلبة. من المفترض، أن كلا البوميرون هما أعمدة Regge. في النهج الحالي، يتم توسيع سعة البوميرون لعمليات الإنتاج الضوئي لبناء سعة لعمليات الإنتاج الكهربائي عن طريق إدخال الكتلة الافتراضية للفوتون  $(Q^2)$  تصبح بقايا القطبين دوال  $Q^2$ . يتم استخراج هذه الدوال عن طريق تركيب المقطع العرضي التفاضلي  $(d\sigma/dt)$  للنموذج الموسع بالطاقة الثابتة  $(w)$  للبيانات التجريبية باستخدام طريقة  $\chi^2$  في كل  $Q^2$ ، يتم ضرب الحدود الصلبة واللينة بالعوامل  $C_0$   $C_1$  لمطابقة البيانات. يتم حساب رؤوس اقتران البوميرون بالجسيمات المتفاعلة من خلال أبعاد الرؤوس التي ترتبط بكتل الجسيمات المتفاعلة في كل قمة.